

Chemical Science

Accepted Manuscript



This is an *Accepted Manuscript*, which has been through the Royal Society of Chemistry peer review process and has been accepted for publication.

Accepted Manuscripts are published online shortly after acceptance, before technical editing, formatting and proof reading. Using this free service, authors can make their results available to the community, in citable form, before we publish the edited article. We will replace this *Accepted Manuscript* with the edited and formatted *Advance Article* as soon as it is available.

You can find more information about *Accepted Manuscripts* in the [Information for Authors](#).

Please note that technical editing may introduce minor changes to the text and/or graphics, which may alter content. The journal's standard [Terms & Conditions](#) and the [Ethical guidelines](#) still apply. In no event shall the Royal Society of Chemistry be held responsible for any errors or omissions in this *Accepted Manuscript* or any consequences arising from the use of any information it contains.



www.rsc.org/chemicalscience



A structural view of synthetic cofactor integration into [FeFe]-hydrogenases

Received 00th January 20xx,
Accepted 00th January 20xx

J. Esselborn^a, N. Muraki^{b†}, K. Klein^c, V. Engelbrecht^a, N. Metzler-Nolte^c, U.-P. Apfel^{c*}, E. Hofmann^d,
G. Kurisu^{b*}, T. Happe^{a*}

DOI: 10.1039/x0xx00000x

www.rsc.org/

[FeFe]-hydrogenases are nature's fastest catalysts for the evolution or oxidation of hydrogen. Numerous synthetic model complexes for the [2Fe] subcluster (2Fe_H) of their active site are known, but so far none of these could compete with the enzymes. The complex Fe₂[μ-(SCH₂)₂X](CN)₂(CO)₄²⁻ with X=NH was shown to integrate into the apo-form of [FeFe]-hydrogenases to yield a fully active enzyme. Here we report the first crystal structures of the apo-form of the bacterial [FeFe]-hydrogenase Cpl from *Clostridium pasteurianum* at 1.60 Å and the active semisynthetic enzyme, Cpl^{ADT}, at 1.63 Å. The structures illustrate the significant changes in ligand coordination upon integration and activation of the [2Fe] complex. These changes are induced by a rigid 2Fe_H cavity as revealed by the structure of apoCpl, which is remarkably similar to Cpl^{ADT}. Additionally we present the high resolution crystal structures of the semisynthetic bacterial [FeFe]-hydrogenases Cpl^{PDT} (X=CH₂), Cpl^{ODT} (X=O) and Cpl^{SDT} (X=S) with changes in the headgroup of the dithiolate bridge in the 2Fe_H cofactor. The structures of these inactive enzymes demonstrate that the 2Fe_H-subcluster and its protein environment remain largely unchanged when compared to the active enzyme Cpl^{ADT}. As the active site shows an open coordination site in all structures, the absence of catalytic activity is probably not caused by steric obstruction. This demonstrates that the chemical properties of the dithiolate bridge are essential for enzyme activity.

Introduction

[FeFe]-hydrogenases are efficient natural catalysts for both the generation and oxidation of H₂¹. This reaction is accomplished by the H-cluster, a metal cofactor consisting of a cubane [4Fe4S] cluster (4Fe_H) connected via a cysteine to an unusual [2Fe] cluster (2Fe_D). The two iron atoms of the latter, termed distal (Fe_d) and proximal (Fe_p) iron are ligated by a total of three CO and two CN⁻ molecules and an aza-dithiolato bridge^{2–5}. Four structural characteristics seem to be important for the high activity of the H-cluster^{6,7}: a) The cyanide ligands besides having additional effects^{8–10} shift the redox potential to more negative values, when compared to all-carbonyl complexes¹¹. b) The 4Fe_H-cluster serves as an intramolecular redox partner^{12–15}. c) A

proton donor is present in the dithiolato bridge^{16–19}. d) The ligand conformation at the 2Fe_H subsite features a CO that bridges or semi-bridges the Fe atoms. This leads to an unoccupied coordination site on Fe_d^{3,5,20–22}. For the hydrogenase HydA1 from *Chlamydomonas reinhardtii* three redox states are discussed as part of the catalytic cycle, which can be distinguished by EPR and FTIR spectroscopy. According to this hypothesis the H-cluster cycles from the H_{ox} state 4Fe_H²⁺-Fe(I)-Fe(II), via the H_{red} state 4Fe_H²⁺-Fe(I)-Fe(I), to the H_{sred} state 4Fe_H¹⁺-Fe(I)-Fe(I). The redox potentials for these transitions are -400 mV and -470 mV vs. SHE close to the H₂/H⁺ redox pair⁷. The crucial proton transfer to and from the active site seems to be accomplished by a proton transfer pathway through the protein towards the central atom of the dithiolato bridge in the 2Fe_H-subcluster^{3,5,23}.

In nature, the 4Fe_H-cluster and other FeS clusters of the enzyme not specific to [FeFe]-hydrogenases are synthesized by the widespread ISC or SUF systems for FeS cluster synthesis yielding inactive hydrogenases, which lack only the specific 2Fe_H-subcluster²⁴. For the sake of simplicity this pre-form will be referred to as apo-form of [FeFe]-hydrogenases throughout this text. The three maturase enzymes HydE, HydF and HydG are necessary for the synthesis of the 2Fe_H-cluster and the assembly of the H-cluster within the protein.²⁵ *In vitro*, chemically synthesized [2Fe] complexes can be bound to the maturase HydF and transferred from there to apo-hydrogenases to form a complete H-cluster.² Notably, also in the absence of HydF or

^aAG Photobiotechnologie, Fakultät für Biologie und Biotechnologie, Ruhr-Universität Bochum, Universitätsstraße 150, 44801 Bochum, Germany. Email: thomas.happe@rub.de.

^bLaboratory of Protein Crystallography, Institute for Protein Research, Osaka University, Suita, Osaka 565-0871, Japan. Email: gkurisu@protein.osaka-u.ac.

^cLehrstuhl für Anorganische Chemie I—Bioanorganische Chemie, Fakultät für Chemie und Biochemie, Ruhr-Universität Bochum, Universitätsstraße 150, 44801 Bochum, Germany. Email: ulf.apfel@rub.de.

^dAG Proteinkristallographie, Fakultät für Biologie und Biotechnologie, Ruhr-Universität Bochum, Universitätsstraße 150, 44801 Bochum, Germany.

[†] Present Addresses: Department of Life and Coordination-Complex Molecular Science, Institute for Molecular Science, National Institutes of Natural Sciences, Okazaki 444-8787, Japan.

Electronic Supplementary Information (ESI) available: [details of any supplementary information available should be included here]. See DOI: 10.1039/x0xx00000x

any other helper protein, an active H-cluster can be formed spontaneously by bringing together the inactive apo-hydrogenase and the chemically synthesized [2Fe] complex $\text{Fe}_2[\mu\text{-(SCH}_2\text{)}_2\text{NH}](\text{CN})_2(\text{CO})_4^{2-}$.²⁶ While the [2Fe] moiety alone is inactive under physiological conditions, the semisynthetic enzyme shows high catalytic activity, which demonstrates the importance of the protein environment. [2Fe] complexes with variations in the dithiolato bridge and/or the other Fe ligands have recently been shown to integrate into HydA1 as well, but the enzymes were inactive or severely limited in their turnover rates especially if the dithiolato bridge was changed.^{2,27} The central atom of the dithiolato-moiety seems to influence the redox behavior of the H-cluster either directly or by interfering with the proton transfer to/from the active site.²⁸

Structures of the active bacterial [FeFe]-hydrogenases^{3,29,30} and the inactive apo-form of HydA1 from *Chlamydomonas reinhardtii*³¹ have been solved at high resolution. In this study we aim to expand the knowledge about maturation of [FeFe]-hydrogenases by reporting the crystal structure of the [FeFe]-hydrogenase from *Clostridium pasteurianum* (Cpl) in its apo-form without the 2Fe_H -cluster (apoCpl). In addition, we contribute to a deeper understanding of [FeFe]-hydrogenase function by solving the structures of four semisynthetic hydrogenases matured in vitro with [2Fe] complexes of the kind $\text{Fe}_2[\mu\text{-(SCH}_2\text{)}_2\text{X}](\text{CN})_2(\text{CO})_4^{2-}$: Fully active Cpl^{ADT} (X=NH) and its non-active derivatives Cpl^{PDT} (X=CH₂), Cpl^{ODT} (X=O) and Cpl^{SDT} (X=S).

Results and discussion

Only an adt-bridged [2Fe] cluster induces H₂ evolution activity in Cpl

To compare the structure of active semisynthetic Cpl containing the adt-bridged 2Fe_H -subcluster with the native bacterial hydrogenase and to investigate potential structural aspects of the impaired function of the semisynthetic enzyme derivatives with different dithiolato bridges, apoCpl was matured with four synthetic [2Fe] clusters. Besides the adt-bridged [2Fe] complex ($\text{Fe}_2[\mu\text{-(SCH}_2\text{)}_2\text{NH}](\text{CN})_2(\text{CO})_4^{2-}$), a pdt-bridged [2Fe] complex ($\text{Fe}_2[\mu\text{-(SCH}_2\text{)}_2\text{CH}_2](\text{CN})_2(\text{CO})_4^{2-}$), an odt-bridged [2Fe] complex ($\text{Fe}_2[\mu\text{-(SCH}_2\text{)}_2\text{O}](\text{CN})_2(\text{CO})_4^{2-}$) and an sdt-bridged [2Fe] complex ($\text{Fe}_2[\mu\text{-(SCH}_2\text{)}_2\text{S}](\text{CN})_2(\text{CO})_4^{2-}$) were synthesized following modified literature procedures^{32–38} and used to prepare semisynthetic Cpl as described before²⁶. Specific hydrogen evolution activities with methylviologen as electron donor were 2874 ± 262 ($\mu\text{mol H}_2$) min^{-1} (mg protein^{-1}) for Cpl with the adt-bridged 2Fe_H -cluster (Cpl^{ADT}), which is in agreement with previously reported values^{10,26}. Neither for apoCpl nor for the non-natural derivatives Cpl^{PDT} , Cpl^{ODT} or Cpl^{SDT} could any hydrogen evolution activity be detected above the detection limit of 0.02% of the activity of Cpl^{ADT} . The same [2Fe] complexes were recently integrated into HydA1. While the odt-bridged and sdt-bridged complexes didn't induce H₂ evolution, 0.9 ($\mu\text{mol H}_2$) min^{-1} (mg protein^{-1}) were reportedly produced by HydA1 with the pdt-bridged 2Fe_H -cluster. This equals 0.17% of the activity of the same enzyme with the

nature-like adt-bridged 2Fe_H -cluster.²⁷ As HydA1 is smaller than Cpl, a better accessibility of the active site from the protein surface might promote undirected proton transfer. This could enable slow H₂ production even though the directed proton transfer via the amine of the 2Fe_H -cluster is disrupted.

All forms of Cpl were crystallized under strictly anaerobic conditions and the crystal structures of both Cpl^{ADT} and apoCpl were solved with molecular replacement using the known structure of active, native Cpl^{ADT} ^{3,30} as a search model and refined to 1.63 Å and 1.60 Å resolution respectively (figure 1, table 1). Cpl^{ADT} was subsequently used as a search model during molecular replacement to determine the structures of Cpl^{PDT} , Cpl^{ODT} and Cpl^{SDT} at 1.82 Å, 1.73 Å and 1.93 Å resolution respectively (figure 1, table 1). In contrast to already known structures of native Cpl^{ADT} ^{3,30,39}, the spacegroup of the crystals was P2₁ for all five enzymes and the asymmetric units each contained two nearly identical molecules. Of these two molecules, one possesses a more flexible N-terminal domain, (residues 1-90), but at the same time a more rigid active site and thus yields a more reliable electron density in the important H-domain in all structures. This becomes evident through the slightly lower temperature factors around the active site when compared to the second molecule. Accordingly figures and values given in the text were taken from the former molecule (chain B) if not stated otherwise, while the complete values for both chains of all structures can be found in the supplemental information.

As in vitro maturation of apo-[FeFe]-hydrogenases with synthetic [2Fe] cofactors was described only recently^{2,26}, we considered the exact structure of the 2Fe_H -cluster and its environment in the semisynthetic enzyme to be of considerable interest. To minimize model bias of electron density in the active site cavity before starting to refine the 2Fe_H -subcluster, at least two rounds of refinement of each structure were performed without a 2Fe_H -cluster in the models.

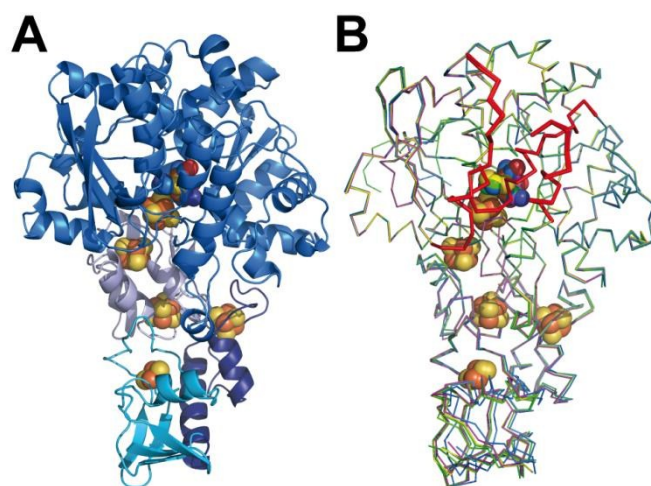


Fig. 1: Structures of unmaturation and semisynthetic [FeFe]-hydrogenases. (A) Cartoon model of [FeFe]-hydrogenase Cpl^{ADT} with domains in different hues of blue. (B) Overlay of ribbon models of [FeFe]-hydrogenases apoCpl (cyan), Cpl^{ADT} (marine), Cpl^{PDT} (magenta), Cpl^{ODT} (green) and Cpl^{SDT} (yellow). H domain regions significantly different to apoHydA1 indicated as thicker ribbon and in red in B. FeS cluster atoms depicted as spheres and colored according to element (Fe=brown, S=beige, O=red, N=blue, C in color of respective protein) in A and B.

	apoCpl	Cpl ^{ADT}	Cpl ^{PDT}	Cpl ^{ODT}	Cpl ^{SDT}
A. Crystallographic data					
X-ray source	SPring8-BL44XU	SLS-PXII	SLS-PXII	SLS-PXII	SLS-PXII
Space group	P2 ₁	P2 ₁	P2 ₁	P2 ₁	P2 ₁
Unit-cell parameters					
a (Å)	90.06	91.34	87.47	89.66	89.83
b (Å)	71.81	73.65	72.07	72.45	73.13
c (Å)	103.31	103.88	102.71	102.94	103.04
Wavelength (Å)	0.900	0.978	0.979	0.979	0.979
Resolution range (Å)	50.00 - 1.60 (1.63 - 1.60) ^a	48.365 - 1.63 (1.67 - 1.63)	47.58 - 1.82 (1.87 - 1.82)	47.77 - 1.73 (1.77 - 1.73)	48.03 - 1.93 (1.98 - 1.93)
Total reflections	645133 (31520)	3729315 (129491)	760236 (56288)	929911 (70575)	674928 (47804)
Unique reflections	172056 (8519)	170277 (12470)	112496 (8270)	136702 (10132)	99824 (7353)
Completeness (%)	99.7% (99.5%)	99.9% (99.7%)	99.9% (100.0%)	100.0% (100.0%)	99.9% (99.9%)
R _{meas} (%)	5.2% (56.5%)	8.7% (109.1%)	14.3% (98.8%)	8.7% (83.1%)	15.8% (93.6%)
I/σ(I)	36.8 (3.2)	20.6(2.2)	9.6 (2.0)	14.1 (2.1)	9.9 (2.1)
Correlation coefficient (CC 1/2) ^b	- (-)	99.9 (87.1)	99.7 (77.9)	99.9 (84.1)	99.6 (68.8)
B. Refinement statistics					
	s				
PDB code	4XDD	4XDC	5BYR	5BYQ	5BYS
Resolution (Å)	1.60	1.63	1.82	1.73	1.93
R _{work}	0.14	0.15	0.16	0.15	0.16
R _{free}	0.17	0.18	0.19	0.18	0.19
No. Atoms (except H)	10548	10385	9859	9978	9991
Protein	9050	9047	8893	8982	8903
Ligand	72	106	106	106	106
Solvent/ion	1426	1232	860	890	982
RMSD from ideal					
Bond lengths (Å)	0.006	0.013	0.018	0.009	0.014
Bond angles (°)	0.95	1.28	1.48	1.07	1.28
Ramachandran plot					
Most favored (%)	97.67	96.90	96.32	97.23	96.59
Additionally allowed (%)	2.33	3.02	3.68	2.77	3.41
Outliers (%)	0.00	0.09	0.00	0.00	0.00
B factors					
overall	35.0	39.0	32.0	35.0	32.0
2FeH cavity (chain A / chain B)	19.5/22.7	24.5/22.0	19.0/16.8	22.3/19.3	18.6/17.3
2FeH (chain A / chain B)	-/-	23.3/20.7	19.3/17.6	23.1/20.2	18.5/17.3
Average occupancy of 2FeH (chain A/ chain B)	-/-	0.98/0.95	0.94/0.96	0.93/0.96	0.98/0.97

^a Numbers in parenthesis represent values for the highest resolution bin.

^b Correlation coefficient CC (1/2) as defined in Karplus and Diederichs 2012.⁵⁵

Subsequently, starting models of the 2Fe_H -subcluster based on the structure of native Cpl³⁰ with optimized geometry but adapted composition of the dithiolato moiety⁵, were used. Restraints were applied to all bond distances in the subcluster. We additionally restrained the angles defining the positions of the CO and CN⁻ ligands. The position of the bridging CO was not restrained due to its reported flexibility⁵ depending on the redox state of the enzyme. Final models of the 2Fe_H subclusters were verified by inspection of composite omit map.

Presumed maturation channel closed in apoCpl crystal structure

The crystal structure of apoCpl reported here is strikingly similar to structures of active Cpl, both native and semisynthetic (figure 1). The overall RMSD of the backbone atoms of apoCpl and native Cpl³⁰ is as low as 0.3 Å, while apoCpl and Cpl^{ADT} display an RMSD of 0.4 Å over all backbone atoms (table S1). Significant differences in side-chain orientation are mainly limited to surface exposed residues with V423 being a notable exception (figure 2). This residue in the central cavity is adapting a different rotamer, supposedly stabilized by one of the water molecules in the binding pocket for 2Fe_H . As demonstrated earlier³¹, the structure of apoHydA1 from *C. reinhardtii* lacking the 2Fe_H -subcluster shows overall great similarity to the structure of the H-domain of Cpl³ and DdH²⁹ with regard to the backbone geometry, but exhibits regions of pronounced differences. Amongst these differences is a channel from the surface to the site of the 2Fe_H -subcluster, which is only present in apoHydA1³¹. Three regions, which can be understood as plug, lock and lid, block the channel in all known structures of active [FeFe]-hydrogenases (figure S1B), while they are remote in apoHydA1. They presumably shift to close the channel and complete the first sphere of amino acid residues around the H-cluster upon integration of the 2Fe_H -subcluster in HydA1³¹ (figure S1A). However, there has neither been a structure of a matured [FeFe]-hydrogenase of the short chlorophyta type nor of an unmaturation bacterial type enzyme, which would have allowed for a direct comparison.

The structure of apoCpl presented here shows the three regions 405-423 ("plug"), 437-453 ("lid") and 529-540 ("lock") clearly in a "closed" conformation nearly identical to active Cpl (figure 1). Prominently, F417 in direct contact to the 2Fe_H -subcluster shows minimal deviation in apoCpl when compared to Cpl^{ADT} (figure 2), while it is moved by 15 Å in apoHydA1. Washed and subsequently dissolved crystals of apoCpl could be matured with the synthetic adt-bridged $[2\text{Fe}]$ cluster to an activity of 1250 nmol $\text{H}_2/\text{min}/\text{crystal}$, reassuring that the reported closed structure of apoCpl is not a dead-end conformation. This suggests an equilibrium between a "closed" and an "open" state in apoCpl, of which only the former readily crystallizes. Within the regions with striking deviation between apoHydA1 and apoCpl, several glycine residues can be identified, which are highly conserved in a recent sequence alignment of all known [FeFe]-hydrogenase sequences⁴⁰ (table S2). These amino acids could function as hinges, as for some of them the "open" or "closed" conformation respectively would imply dihedral angle combinations commonly found only for glycine residues⁴¹ (table S2). Their high degree of conservation thus is another hint that an open and closed form of all [FeFe]-hydrogenases exists.

Rigid cavity in apoCpl forces the $[2\text{Fe}]$ complex to move into its active conformation

Being devoid of the 2Fe_H -cluster, the active site binding pocket of apoCpl is occupied by seven water molecules and a chloride ion (figure 2) instead. Note that this leaves a water filled cavity of roughly 10 Å diameter in the center of the protein. Nonetheless, residues which are assumed to interact with the cofactor in the active enzyme are shifted only very slightly by 0.1-0.3 Å towards a narrower cavity (table S3, figure 2) and show the same low temperature factors as most of the H-domain (table 1). This exemplifies how the amino acids of seven distinct protein parts (around amino acids 231, 299, 324, 353, 417, 497 and 503; figure 3) coordinate to form a rigid

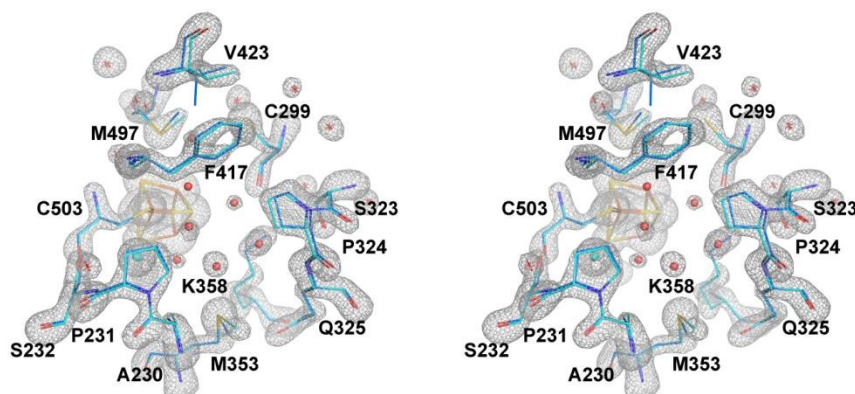


Fig. 2: The central cavity of apoCpl and Cpl^{ADT}. Stereo view of a stick model of the central cavity of apoCpl (carbon atoms in cyan) with Fo-Fc simulated annealing omit map contoured at 4σ in the identical orientation as Figure 3. A stick model of amino acids lining the central cavity of Cpl^{ADT} is superposed (carbon atoms in marine). Numbering of amino acids as in the structure of native Cpl. Small spheres indicate water atoms (red) and chloride ion (cyan) not present in Cpl^{ADT}.

central cavity, perfectly positioned to arrange the ligands of a [2Fe] cluster in its center.

Crystal structure of semisynthetic Cpl^{ADT} reveals native-like structure and open coordination site

Superposition of the structure of semisynthetic Cpl^{ADT} and the best available crystal structure of native Cpl³⁰ results in nearly identical structures with an RMSD of 0.3 Å for the main chain atoms. Even with regard to the side chain atom conformations, significant differences between Cpl^{ADT} and the native Cpl can only be found in several surface exposed residues, which is surprising given the considerable differences in the crystal packing.

When comparing the important cofactor-peptide interactions in native Cpl and the structure of Cpl^{ADT}, the distances between the atoms of 2Fe_H and their respective interaction partners in the protein environment show a maximum deviation of 0.17/0.13 Å and an average deviation of 0.06/0.05 Å for chain A/chain B (figure 3, table S4). This is well within the experimental error of crystal structure analysis at the given resolution. Moreover the synthetic 2Fe_H-cluster itself in the structure of Cpl^{ADT} compares very well to the *in vivo* synthesized version in native Cpl³⁰ (figure 3) and the [FeFe]-hydrogenases DdH²⁹ and HydA1 (data from XANES/EXAFS)⁴² within the error of crystal structures of macromolecules (table S5). This finding confirms data from FTIR and EPR spectroscopic studies, which showed excellent agreement of native and semisynthetic protein for the small [FeFe]-hydrogenase HydA1 from *Chlamydomonas reinhardtii*^{26,28}. For [FeFe]-hydrogenases with additional N-terminal domains like Cpl or DdH, a bridging conformation of one CO ligand is assumed to occur only in the H_{ox} or CO inhibited state^{5,21,29}. In our structure the CO ligand between the Fe atoms is positioned at an angle of 114°/132° (chain A /chain B) between Fe_d-C-O (table S5, figure 4), which does not indicate terminal binding of the CO to Fe_d as previously published for a structure of reduced DdH⁵. Thus we understand the here reported structure of Cpl^{ADT} to be mainly in the H_{ox} state. While in earlier structures of Cpl^{3,30} a region of low but significant electron density next to Fe_d was assigned as a water molecule in this particular redox state, in the structure described here the H-cluster of both chains clearly features one coordination site on Fe_d devoid of electron density (figure 4).

A comparison of the crystal structures of the synthetic adt-bridged [2Fe] complex³⁷ before and after integration into the protein environment as 2Fe_H illustrates the distortions that the protein forces upon the [2Fe] complex (figure 4). An Fe-S-Fe bridge to the 4Fe_H-cluster is formed and, as demonstrated earlier, one CO ligand is lost during the process of activation²⁶. Another CO ligand shifts into a bridging position between the two Fe atoms and the CO/CN⁻ ligands move into an octahedral coordination at each Fe with nearly perpendicular equatorial planes (figure 4). This conformation has been attributed a crucial role in allowing the mixed Fe(I)-Fe(II) valency of the H_{ox} state within the catalytic cycle, which is difficult to achieve in isolated [2Fe] clusters⁴³. Additionally the new conformation features the open

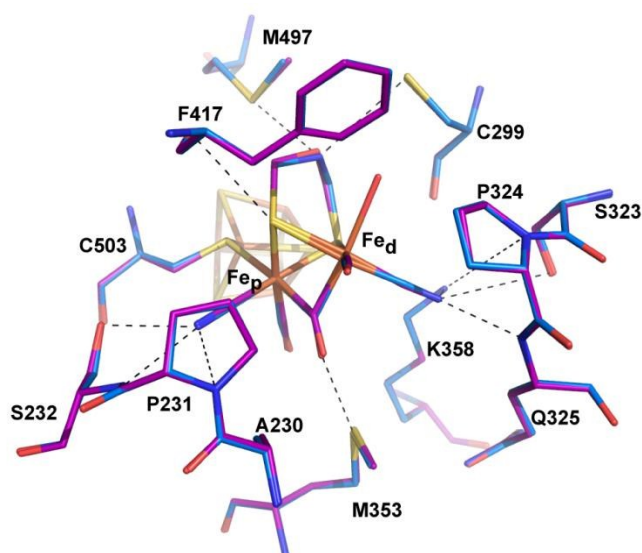
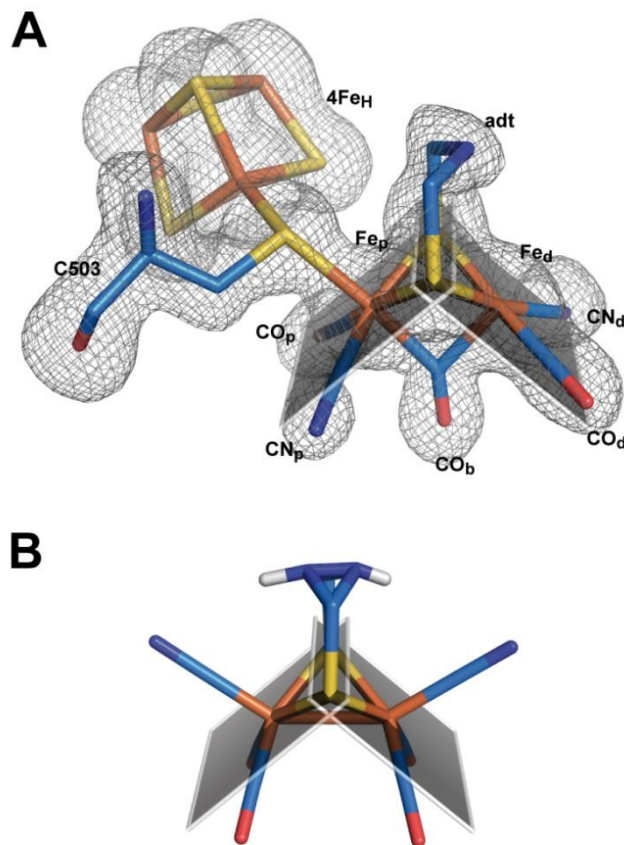


Fig. 3: Comparison of the active site of Cpl^{ADT} and native Cpl. Stick model of the environment of the 2Fe_H-subcluster of Cpl^{ADT} (carbon atoms in marine) superposed to a stick model of native Cpl (PDB ID 3C8Y)³⁰ (carbon atoms in magenta). Dashed lines indicate potential interactions between 2Fe_H and the protein listed in table S4. Numbering of amino acids as in the structure of native Cpl.

Fig. 4: Structure of semisynthetic H-cluster and structural changes in ligand coordination upon integration of 2Fe_H. (A) Stick model of the H-cluster of Cpl^{ADT} colored according to element with F_o-F_c simulated annealing omit map contoured at 3.5σ. (B) Stick model of the crystal structure of Fe₂[μ-(SCH₂)₂NH](CN)₂(CO)₄²⁻³⁷. The planes in A and B are drawn through the sulfur atoms of the [2Fe] complexes and one of the two Fe atoms each to clarify the coordination geometry of the Fe ligands.



coordination site at Fe_d trans to the bridging CO (figure 4). This promotes regioselectivity of H_2 binding or hydride formation close to the amine in the *adt*-bridge, which is believed to be crucial for the mechanism^{16,44}.

2Fe_H subsite structure remains unaltered upon changes in the dithiolato bridge

The structures of all three Cpl derivatives with non-natural 2Fe_H subsites superpose very well with each other and the native Cpl, apoCpl and Cpl^{ADT} with RMSD's for C_α atoms between 0,2 Å and 0,5 Å (table S1). Comparison of the exact positions of amino acids supposedly involved in enzyme function, e.g. amino acids in the proton transfer pathway or around the active site, yielded little differences within the limits of exactness of macromolecular crystallography (figure 5). The average RMSDs of all atoms of selected amino acids were as low as 0.08-0.11 Å when comparing the non-natural derivatives with Cpl^{ADT}. As significant differences in the degree of maturation were observed for semisynthetic HydA1 with non-natural 2Fe_H clusters²⁷, we allowed variation of the occupancies of the atoms of the 2Fe_H -subclusters during refinement. According to this rough estimate more than 90% of the molecules in the crystals contained the 2Fe_H subsite (table 1). Even though the effects of partial occupancy and temperature factor are hardly discernible at the given resolution, we expect these results to be a good lower limit as the calculated temperature factors of the 2Fe_H -clusters and the surrounding amino acids agree well (table 1).

As apoCpl crystallizes in a nearly identical structure and an isomorphous unit cell we assume that the high occupancy of the 2Fe_H -clusters does not result from positive selection during crystal formation, but illustrates the effectiveness of *in vitro* maturation of Cpl with the chosen $[2\text{Fe}]$ clusters.

For the *odt*-bridged 2Fe_H subsite in HydA1 a less pronounced bridging character of CO_b compared to other semisynthetic HydA1 enzymes was reported according to FTIR data of the "as isolated" state.²⁷ A very similar state represented a minor part of the mixed population of HydA1 with *sdt*-bridged 2Fe_H -subcluster in the same study. We found an angle of 145° between Fe_d -C-O of the CO_b ligand in Cpl^{SDT} which indicates a more terminal than bridging character, but the other structures including Cpl^{ODT} reveal angles suggesting a bridging CO (figure 6, table S5).

Because of the above discussed effects of redox state changes on the CO_b ligand, a potential dependent FTIR based investigation of the Cpl enzyme derivatives would be needed to clarify if this is merely an effect of the redox state at the point of crystal mounting or inherent to the different dithiolato bridge. A detailed comparison of distances between the atoms of the 2Fe_H subsite and the surrounding amino acids indicates a slightly different position of Fe_d within the cavity for Cpl^{PDT} 0.1 Å closer to Ala 230 and further away from Cys 299 (table S4). Besides this, small differences in the dithiolato bridge can be observed. While the bridgehead atom is leaning about 0.2 Å further away from Met 497 in the inactive Cpl

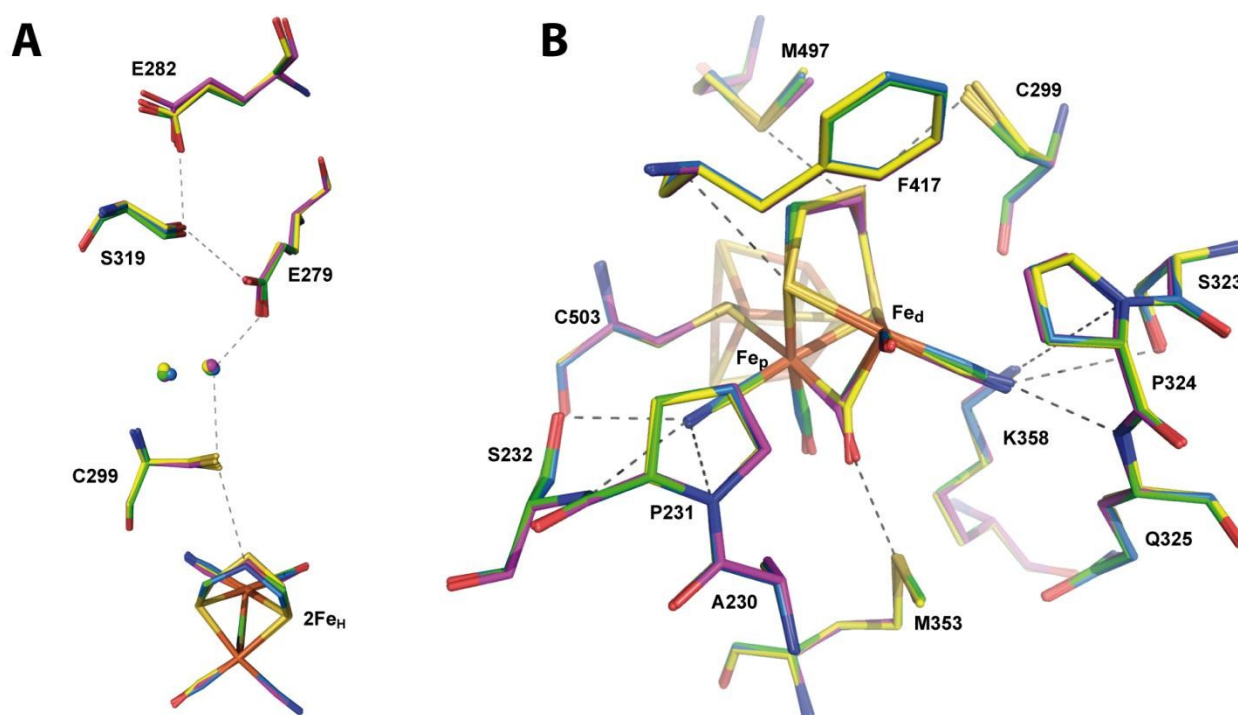


Fig. 5: Comparison of the catalytically important amino acids in Cpl derivatives. Stick models of the potential proton transfer pathway (A) and the environment of the 2Fe_H -subcluster (B) of Cpl^{ADT} (carbon atoms in marine) superposed to stick models of Cpl^{PDT} (magenta), Cpl^{ODT} (green) and Cpl^{SDT} (yellow). Dashed lines indicate potential proton transfer interactions or potential interactions of 2Fe_H with the protein as listed in table S4. Numbering of amino acids as in the structure of native Cpl.

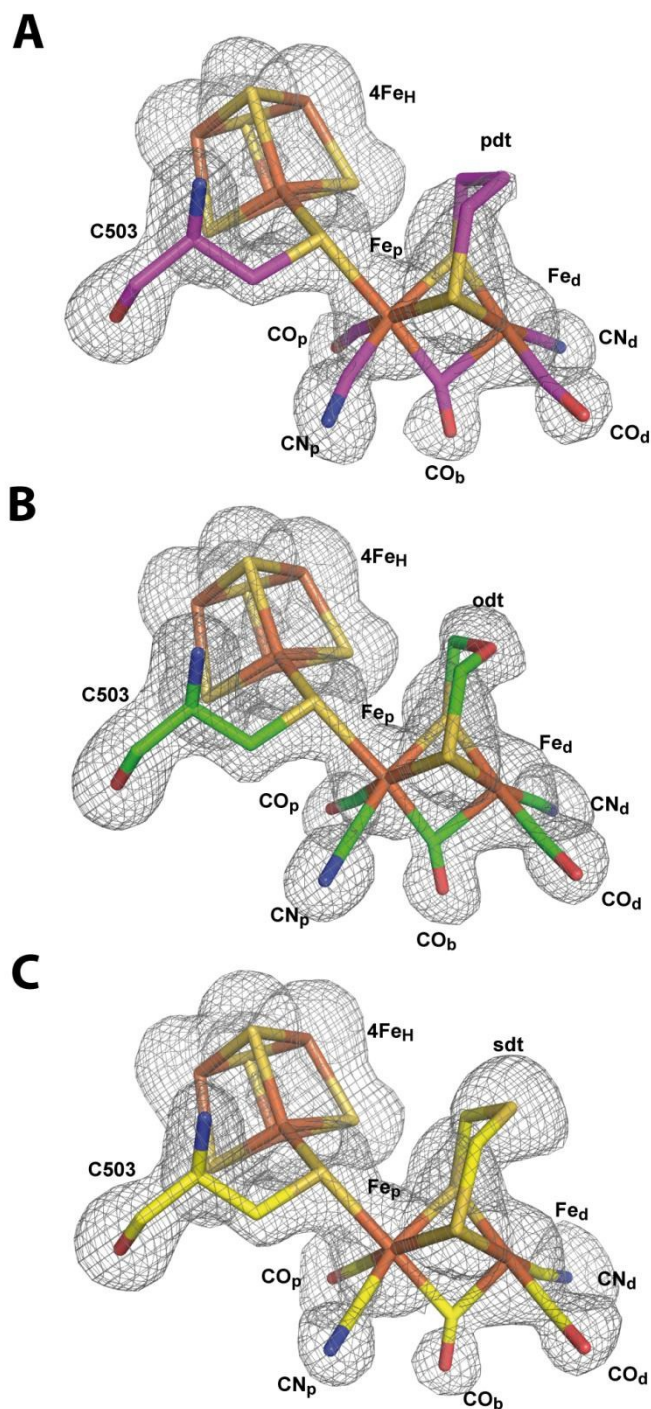


Fig. 6: Models of the H-cluster of non-native Cpl derivatives. Stick models of (A) Cpl^{PDT} (carbon atoms in magenta), (B) Cpl^{ODT} (carbon atoms in green) and (C) Cpl^{SDT} (carbon atoms in yellow) with F_o-F_c simulated annealing omit maps contoured at 3.5 σ .

derivatives, the sulfur atom of Cys 299 is pushed back to keep roughly the van-der-Waals distance to the bridgehead atom of the dithiolato bridge in the three structures (figure 5B, table S3). However, the position and geometry of the non-natural 2Fe_H-clusters do not show any large differences (figure 5, figure 6, table S5) when compared to native Cpl or Cpl^{ADT} and thus do not offer a clear structural explanation for the impaired activity. For Cpl^{PDT} this is in line with a recent ENDOR and HYSCORE study of HydA1 containing a pdt-bridged 2Fe_H-subcluster, which

showed very similar spectra in comparison to *in vivo* matured DdH.⁴⁵ DFT calculations performed for adt-bridged, pdt-bridged and odt-bridged 2Fe_H-subclusters in Cpl also resulted in very similar geometries³⁰ (table S5). Remarkably, there is no significant electron density in our structures close to Fe_d at the postulated site of H₂ binding in any of the 2Fe_H-subclusters (figure 6). Thus binding of an inhibitor to this open coordination site can be ruled out as cause for the quantitative loss of activity. For HydA1 with the pdt-bridged 2Fe_H cluster no binding of CO to the active site was observed in a recent FTIR based study.²⁸ Our structure of Cpl^{PDT} rules out a rearrangement in the neighboring amino acids as explanation for this behavior. However, once an inhibitory CO is bound to Fe_d, the distance between the central atom of the dithiolate bridge and the oxygen of CO was reported to be as close as ~ 2.5 Å.⁵ While the single hydrogen of an amine bridgehead proposedly points towards C299 and thus away from Fe_d, the pdt's central methyl group might considerably obstruct binding of CO to Fe_d through its hydrogen atoms not visible in X-ray crystallography at the given resolution.

Conclusions

We herein report the structure of the [FeFe]-hydrogenase Cpl from *Clostridium pasteurianum* in the unmaturation apo-form and the first high resolution structure of a fully active semisynthetic [FeFe]-hydrogenase along with the structures of three non-natural inactive derivatives of this [FeFe]-hydrogenase with changes in the inorganic active site. Surprisingly, the unmaturation apoCpl crystallizes in an overall conformation like the matured enzyme and not similar to the structure of unmaturation HydA1. The high degree of rigidity of the amino acids in proximity to the H-cluster even in the absence of the 2Fe_H-subcluster demonstrates how the protein structure is designed to force the 2Fe-cofactor into its highly active form. Semisynthetic Cpl^{ADT} shows a nearly identical conformation when compared to the native enzyme including the rotated conformation of the 2Fe_H cofactor with octahedral geometry at both Fe atoms. Unlike previous structures of Cpl, the structure of Cpl^{ADT} presented here displays a completely unoccupied open coordination site at Fe_d. Non-natural derivatives of the 2Fe_H subsite with changes in the central atom of the dithiolato bridge can well be incorporated into apoCpl as already reported for apoHydA1, but do not lead to H₂ evolution activity. The structures of the protein matrix of Cpl^{PDT}, Cpl^{ODT} and Cpl^{SDT} show no clear differences to the highly active Cpl^{ADT}. Despite their divergence in activity all four different 2Fe_H-subclusters investigated in this study are adapted in their conformation to the protein matrix when compared to the structures of the free [2Fe] complexes and take up the same typical structure. The proposed site of H₂ oxidation at Fe_d is unoccupied in all structures reported here, which excludes inhibitor binding or steric hindrance as reasons for impaired activity. The structural information gained in this study in combination with previously reported FTIR^{27,28} and EPR⁴¹ spectroscopic data of inactive active site variants of [FeFe]-hydrogenases underline the central role the chemistry of the dithiolato bridge plays for enzyme activity. Once the protein

environment has forced the iron ligands into the typical conformation, which is the basis of H₂ evolution, it is solely the reactivity of the central amine, which induces enzyme activity.

Experimental Section

ApoCpl was expressed with a C-terminally fused strep-tagII in E.c. BL21(DE3) ΔiscR⁴⁶ under anaerobic conditions as described earlier⁴⁷ without coexpression of [FeFe]-hydrogenase specific maturases. Protein purification was achieved by strep-tactin affinity chromatography under strictly anaerobic conditions⁴⁸ with a 10 mM Tris-HCl buffer with pH 8.0 and 2 mM NaDT and purity was assessed by SDS-PAGE.

[Fe₂[μ-(SCH₂)₂NH](CN)₂(CO)₄][Et₄N]₂ was synthesized as reported earlier². As the purification of [Fe₂[μ-(SCH₂)₂NH](CN)₂(CO)₄][Et₄N]₂ by washing with hexane³⁴ did not result in clean product, the recently described purification procedure for [Fe₂[μ-(SCH₂CH₂CH₂S)](CN)₂(CO)₄][Et₄N]₂² was adopted for [Fe₂[μ-(SCH₂)₂NH](CN)₂(CO)₄][Et₄N]₂.

[Fe₂[μ-(SCH₂CH₂CH₂S)](CN)₂(CO)₄][Et₄N]₂, [Fe₂[μ-(SCH₂)₂S](CN)₂(CO)₄][Et₄N]₂ and [Fe₂[μ-(SCH₂)₂O](CN)₂(CO)₄][Et₄N]₂ were synthesized according to literature procedures^{33,35,36,38} and purity of each sample was checked by ¹H NMR and IR spectroscopy. Samples were stored at -35°C under inert atmosphere to avoid any decomposition of the artificial cofactors.

Maturation of apoCpl to Cpl^{ADT}, Cpl^{PDT}, Cpl^{ODT} or Cpl^{SDT} with a 10fold excess of Fe₂[μ-(SCH₂)₂X](CN)₂(CO)₄][Et₄N]₂ was achieved in a 0.1 M K₂HPO₄/KH₂PO₄ buffer system at pH 6.8 with 2 mM NaDT as described earlier²⁶ at RT for 1 hour to ensure complete maturation of the sample. The semisynthetic enzymes were subsequently cleaned from leftover [2Fe] complex and buffered again into a 10 mM Tris-HCl buffer with pH 8.0 and 2 mM NaDT by use of a NAP[™] 5 (GE Healthcare) size exclusion chromatography column. Enzyme preparations were concentrated using Amicon Ultra centrifugal filters 30K (Millipore) under anaerobic conditions. Success of maturation and quality of purified protein samples of Cpl^{ADT} were determined by testing their H₂ production activity *in vitro* with methylviologen as electron donor using an established method⁴⁹. To test for catalytic activity of the non-native semisynthetic enzymes, the same method was applied and additional measurements with 10fold increased protein amount were conducted to lower the limit of detection.

Box-like protein crystals of apoCpl and the semisynthetic hydrogenases were obtained with PEG 3000 or PEG 4000 as precipitant using the hanging drop or sitting drop vapor diffusion method at 277 K under anaerobic conditions within 2-4 days when mixing reservoir solution 1:1 with protein solution (10 mg/ml). The crystallization conditions for the selected crystals of apoCpl were 12% PEG 3000, 0.1 M MES pH 6.5, 0.2 M MgCl₂ in a sitting drop vapor diffusion experiment and cryo-protection was achieved with a final concentration of 15% glycerol in 15% PEG 3000, pH 6.5, 0.2M MgCl₂. Cpl^{ADT} crystals selected for diffraction experiments were grown in 11% PEG 4000, 0.1 M MES pH 7.0, 0.2 M MgCl₂ in a hanging drop experiment and protected against formation of ice crystals with paraffin oil. Crystals of the non-native semisynthetic enzymes

were grown by hanging drop vapor diffusion using 0.1 M MES pH 6.0, 0.4 M MgCl₂ and a total of 40% v/v of PEG4000 and glycerol to avoid the need of additional cryo-protection during crystal mounting. In detail the reservoir solutions contained 15% PEG 4000, 25% glycerol for Cpl^{PDT}, 19% PEG 4000, 21% glycerol for Cpl^{ODT} and 21% PEG 4000, 19% glycerol for Cpl^{SDT}. Maturation capability of crystallized apoCpl was tested by washing a crystal in three fresh drops of its reservoir solution followed by dissolution of the crystal in cold 0.1 M K₂HPO₄/KH₂PO₄ buffer at pH 6.8 with 2 mM NaDT under strictly anaerobic conditions. Maturation was started by addition of 1.5 pmol Fe₂[μ-(SCH₂)₂NH](CN)₂(CO)₄][Et₄N]₂ in 0.1 M K₂HPO₄/KH₂PO₄ buffer, pH 6.8, and allowed to proceed for 1 h at 4°C. Subsequently the mixture was transferred completely into a solution of methylviologen, NaDT and phosphate buffer as for standard tests for H₂ evolution activity and treated accordingly⁴⁹.

Mounting of protein crystals into CryoLoops[™] (Hampton Research) and subsequent flash-freezing in liquid N₂ was performed under strictly anaerobic conditions at 298 K. Diffraction data were collected at 100 K at beamline BL44-XU at SPring-8 (Hyogo, Japan) and beamline PXII at the SLS (Villingen, Switzerland) and the data were processed using the software package HKL2000⁵⁰ and XDS⁵¹ for apoCpl and the semisynthetic hydrogenases, respectively. Molecular replacement and structure optimization were performed with the software packages CCP4⁵² (apoCpl and Cpl^{ADT}) and PHENIX⁵³ (Cpl^{PDT}, Cpl^{ODT} and Cpl^{SDT}) and Coot⁵⁴. At least two final refinement runs were conducted with PHENIX on all structures to improve comparability of the final models. In order to estimate the occupancy of the 2Fe_H-cluster in the structures of Cpl^{ADT} and other derivatives, we applied a partial occupancy refinement at the final stage of PHENIX refinement. Simulated annealing omit maps were calculated with PHENIX, omitting the H-cluster with the bridging cysteine residue and the residues around the central cavity as well as all atoms within the central cavity for the semisynthetic [FeFe]-hydrogenases and apoCpl, respectively.

Acknowledgements

We thank the staff at beam line PXII at SLS, Switzerland, and BL44XU at SPring-8, Japan, and at the ESRF, France, for their help during data collection.

Notes and references

Funding sources

This work was supported in part by an International Joint Research Promotion Program, Osaka University, (G.K, T.H.); the Cabinet Office of Japan, through the Funding Program for Next Generation World-Leading Researchers (NEXT Program) (GS016, to G.K.) and the Studienstiftung des deutschen Volkes (J.E.). U.-P.A. was supported by the Fonds of the Chemical Industry (Liebig grant) and the Deutsche Forschungsgemeinschaft (Emmy Noether grant AP242/2-1).

T.H. thanks the Cluster of Excellence RESOLV (EXC1069) funded by the Deutsche Forschungsgemeinschaft (DFG) and the Volkswagen Foundation (LigH2t).

The authors declare no competing financial interest.

Accession Numbers

The coordinates and structure factors for all structures were deposited with the Protein Data Bank under the following accession numbers: apoCpl: 4XDD, Cpl^{ADT}: 4XDC, Cpl^{PDT}: 5BYR, Cpl^{ODT}: 5BYQ, Cpl^{SdT}: 5BYS.

Abbreviations

2Fe_H, [2Fe] subcluster of the H-cluster of [FeFe]-hydrogenases; 4Fe_H, [4Fe4S] subcluster of the H-cluster; adt, aza -dithiolate; apoCpl, Cpl lacking only the 2Fe_H-cluster; Cpl, [FeFe]-hydrogenase I from *Clostridium pasteurianum*; Cpl^{ADT}, apoCpl matured in vitro with (Fe₂[μ-(SCH₂)₂NH](CN)₂(CO)₄²⁻); Cpl^{ODT}, apoCpl matured in vitro with (Fe₂[μ-(SCH₂)₂O](CN)₂(CO)₄²⁻); Cpl^{PDT}, apoCpl matured in vitro with (Fe₂[μ-(SCH₂)₂CH₂](CN)₂(CO)₄²⁻); Cpl^{SdT}, apoCpl matured in vitro with (Fe₂[μ-(SCH₂)₂S](CN)₂(CO)₄²⁻); DdH, [FeFe]-hydrogenase from *Desulfovibrio desulfuricans*; HydA1, [FeFe]-hydrogenase I from *Chlamydomonas reinhardtii*; odt, oxo -dithiolate; pdt, propane-dithiolate; sdt, sulfur-dithiolate.

Supporting Information

Tables listing and comparing the RMSD of the structures, distances and angles of the 2Fe_H-subclusters, the distances from 2Fe_H-subcluster atoms to selected amino acids and the distances of amino acids lining the 2Fe_H-subcluster cavity, a figure showing the presumed maturation channel in more detail and additional information on the suggested glycine hinges and stereo views of all figures presented in the main article.

References

- M. Frey, *ChemBioChem*, 2002, **3**, 153–160.
- G. Berggren, A. Adamska, C. Lambertz, T. R. Simmons, J. Esselborn, M. Atta, S. Gambarelli, J.-M. Mouesca, E. Reijerse, W. Lubitz, T. Happe, V. Artero and M. Fontecave, *Nature*, 2013, **499**, 66–69.
- J. W. Peters, W. N. Lanzilotta, B. J. Lemon and L. C. Seefeldt, *Science*, 1998, **282**, 1853–1858.
- A. Silakov, B. Wenk, E. Reijerse and W. Lubitz, *Phys. Chem. Chem. Phys.*, 2009, **11**, 6592.
- Y. Nicolet, A. L. de Lacey, X. Vernède, V. M. Fernandez, E. C. Hatchikian and J. C. Fontecilla-Camps, *J. Am. Chem. Soc.*, 2001, **123**, 1596–1601.
- T. R. Simmons, G. Berggren, M. Bacchi, M. Fontecave and V. Artero, *Coord. Chem. Rev.*, 2014, **270–271**, 127–150.
- W. Lubitz, H. Ogata, O. Rüdiger and E. Reijerse, *Chem. Rev.*, 2014, **114**, 4081–4148.
- C. A. Boyke, J. I. van der Vlugt, T. B. Rauchfuss, S. R. Wilson, G. Zampella and L. De Gioia, *J. Am. Chem. Soc.*, 2005, **127**, 11010–11018.
- M. Bruschi, C. Greco, L. Bertini, P. Fantucci, U. Ryde and L. D. Gioia, *J. Am. Chem. Soc.*, 2010, **132**, 4992–4993.
- P. Knörzer, A. Silakov, C. E. Foster, F. A. Armstrong, W. Lubitz and T. Happe, *J. Biol. Chem.*, 2012, **287**, 1489–1499.
- G. A. N. Felton, C. A. Mebi, B. J. Petro, A. K. Vannucci, D. H. Evans, R. S. Glass and D. L. Lichtenberger, *J. Organomet. Chem.*, 2009, **694**, 2681–2699.
- J. M. Camara and T. B. Rauchfuss, *Nat. Chem.*, 2012, **4**, 26–30.
- C. Tard, X. Liu, S. K. Ibrahim, M. Bruschi, L. D. Gioia, S. C. Davies, X. Yang, L.-S. Wang, G. Sawers and C. J. Pickett, *Nature*, 2005, **433**, 610–613.
- C. Greco, *Inorg. Chem.*, 2013, **52**, 1901–1908.
- C. Greco, M. Bruschi, P. Fantucci, U. Ryde and L. De Gioia, *Chemphyschem Eur. J. Chem. Phys. Phys. Chem.*, 2011, **12**, 3376–3382.
- M. Bruschi, C. Greco, M. Kaukonen, P. Fantucci, U. Ryde and L. De Gioia, *Angew. Chem. Int. Ed.*, 2009, **48**, 3503–3506.
- M. E. Carroll, B. E. Barton, T. B. Rauchfuss and P. J. Carroll, *J. Am. Chem. Soc.*, 2012, **134**, 18843–18852.
- S. Ezzaher, A. Gogoll, C. Bruhn and S. Ott, *Chem. Commun.*, 2010, **46**, 5775–5777.
- N. Wang, M. Wang, L. Chen and L. Sun, *Dalton Trans.*, 2013, **42**, 12059–12071.
- C.-H. Hsieh, O. F. Erdem, S. D. Harman, M. L. Singleton, E. J. Reijerse, W. Lubitz, C. V. Popescu, J. H. Reibenspies, S. M. Brothers, M. B. Hall and M. Y. Darensbourg, *J. Am. Chem. Soc.*, 2012.
- W. Roseboom, A. L. Lacey, V. M. Fernandez, E. C. Hatchikian and S. P. J. Albracht, *JBIC J. Biol. Inorg. Chem.*, 2006, **11**, 102–118.
- A. Silakov, C. Kamp, E. Reijerse, T. Happe and W. Lubitz, *Biochemistry (Mosc.)*, 2009, **48**, 7780–7786.
- A. J. Cornish, K. Gartner, H. Yang, J. W. Peters and E. L. Hegg, *J. Biol. Chem.*, 2011, **286**, 38341–38347.
- D. W. Mulder, D. O. Ortillo, D. J. Gardenghi, A. V. Naumov, S. S. Ruebush, R. K. Szilagyi, B. Huynh, J. B. Broderick and J. W. Peters, *Biochemistry (Mosc.)*, 2009, **48**, 6240–6248.
- E. M. Shepard, F. Mus, J. N. Betz, A. S. Byer, B. R. Duffus, J. W. Peters and J. B. Broderick, *Biochemistry (Mosc.)*, 2014, **53**, 4090–4104.
- J. Esselborn, C. Lambertz, A. Adamska-Venkatesh, T. Simmons, G. Berggren, J. Noth, J. Siebel, A. Hemschemeier, V. Artero, E. Reijerse, M. Fontecave, W. Lubitz and T. Happe, *Nat. Chem. Biol.*, 2013, **9**, 607–609.
- J. F. Siebel, A. Adamska-Venkatesh, K. Weber, S. Rumpel, E. J. Reijerse and W. Lubitz, *Biochemistry (Mosc.)*, 2015, **54**, 1474–1483.
- A. Adamska-Venkatesh, D. Krawietz, J. Siebel, K. Weber, T. Happe, E. Reijerse and W. Lubitz, *J. Am. Chem. Soc.*, 2014, **136**, 11339–11346.
- Y. Nicolet, C. Piras, P. Legrand, C. E. Hatchikian and J. C. Fontecilla-Camps, *Structure*, 1999, **7**, 13–23.
- A. S. Pandey, T. V. Harris, L. J. Giles, J. W. Peters and R. K. Szilagyi, *J. Am. Chem. Soc.*, 2008, **130**, 4533–4540.
- D. W. Mulder, E. S. Boyd, R. Sarma, R. K. Lange, J. A. Endrizzi, J. B. Broderick and J. W. Peters, *Nature*, 2010, **465**, 248–251.
- E. J. Lyon, I. P. Georgakaki, J. H. Reibenspies and M. Y. Darensbourg, *Angew. Chem. Int. Ed.*, 1999, **38**, 3178–3180.
- A. L. Cloirec, S. C. Davies, D. J. Evans, D. L. Hughes, C. J. Pickett, S. P. Best and S. Borg, *Chem. Commun.*, 1999, **22**, 2285–2286.
- M. Schmidt, S. M. Contakes and T. B. Rauchfuss, *J. Am. Chem. Soc.*, 1999, **121**, 9736–9737.
- L.-C. Song, Z.-Y. Yang, Y.-J. Hua, H.-T. Wang, Y. Liu and Q.-M. Hu, *Organometallics*, 2007, **26**, 2106–2110.
- J. Windhager, H. Görls, H. Petzold, G. Mloston, G. Linti and W. Weigand, *Eur. J. Inorg. Chem.*, 2007, **2007**, 4462–4471.
- H. Li and T. B. Rauchfuss, *J. Am. Chem. Soc.*, 2002, **124**, 726–727.
- L.-C. Song, Z.-Y. Yang, H.-Z. Bian, Y. Liu, H.-T. Wang, X.-F. Liu and Q.-M. Hu, *Organometallics*, 2005, **24**, 6126–6135.
- B. J. Lemon and J. W. Peters, *Biochemistry (Mosc.)*, 1999, **38**, 12969–12973.
- M. Winkler, J. Esselborn and T. Happe, *Biochim. Biophys. Acta BBA - Bioenerg.*, 2013, **1827**, 974–985.

- 41 S. C. Lovell, I. W. Davis, W. B. Arendall, P. I. W. de Bakker, J. M. Word, M. G. Prisant, J. S. Richardson and D. C. Richardson, *Proteins Struct. Funct. Bioinforma.*, 2003, **50**, 437–450.
- 42 C. Lambertz, P. Chernev, K. Klingan, N. Leidel, K. G. V. Sigfridsson, T. Happe and M. Haumann, *Chem. Sci.*, 2014, **5**, 1187–1203.
- 43 T. Liu and M. Y. Darensbourg, *J. Am. Chem. Soc.*, 2007, **129**, 7008–7009.
- 44 V. Fourmond, C. Greco, K. Sybirna, C. Baffert, P.-H. Wang, P. Ezanno, M. Montefiori, M. Bruschi, I. Meynial-Salles, P. Soucaille, J. Blumberger, H. Bottin, L. De Gioia and C. Léger, *Nat. Chem.*, 2014, **6**, 336–342.
- 45 A. Adamska-Venkatesh, T. R. Simmons, J. F. Siebel, V. Artero, M. Fontecave, E. Reijerse and W. Lubitz, *Phys. Chem. Chem. Phys.*, 2015, **17**, 5421–5430.
- 46 M. K. Akhtar and P. R. Jones, *Appl. Microbiol. Biotechnol.*, 2008, **78**, 853–862.
- 47 J. M. Kuchenreuther, C. S. Grady-Smith, A. S. Bingham, S. J. George, S. P. Cramer and J. R. Swartz, *PLoS ONE*, 2010, **5**.
- 48 G. von Abendroth, S. Stripp, A. Silakov, C. Croux, P. Soucaille, L. Girbal and T. Happe, *Int. J. Hydrog. Energy*, 2008, **33**, 6076–6081.
- 49 A. Hemschemeier, A. Melis and T. Happe, *Photosynth. Res.*, 2009, **102**, 523–540.
- 50 Z. Otwinowski and W. Minor, *Macromol. Crystallogr. Pt A*, 1997, **276**, 307–326.
- 51 W. Kabsch, *Acta Crystallogr. D Biol. Crystallogr.*, 2010, **66**, 125–132.
- 52 M. D. Winn, C. C. Ballard, K. D. Cowtan, E. J. Dodson, P. Emsley, P. R. Evans, R. M. Keegan, E. B. Krissinel, A. G. W. Leslie, A. McCoy, S. J. McNicholas, G. N. Murshudov, N. S. Pannu, E. A. Potterton, H. R. Powell, R. J. Read, A. Vagin and K. S. Wilson, *Acta Crystallogr. D Biol. Crystallogr.*, 2011, **67**, 235–242.
- 53 P. D. Adams, P. V. Afonine, G. Bunkóczi, V. B. Chen, I. W. Davis, N. Echols, J. J. Headd, L.-W. Hung, G. J. Kapral, R. W. Grosse-Kunstleve, A. J. McCoy, N. W. Moriarty, R. Oeffner, R. J. Read, D. C. Richardson, J. S. Richardson, T. C. Terwilliger and P. H. Zwart, *Acta Crystallogr. D Biol. Crystallogr.*, 2010, **66**, 213–221.
- 54 P. Emsley, B. Lohkamp, W. G. Scott and K. Cowtan, *Acta Crystallogr. D Biol. Crystallogr.*, 2010, **66**, 486–501.
- 55 P. A. Karplus and K. Diederichs, *Science*, 2012, **336**, 1030–1033.